Humidity-induced self-assembled nanostructures via ion aggregation in ionic linear polysiloxanes

Mitsuo Hara[1], Atsuki Kodama[1], Shohei Washiyama[1], Yoshihisa Fujii[2], Shusaku Nagano[3], and Takahiro Seki*[1]*

[1] Department of Molecular and Macromolecular Chemistry, Graduate School of Engineering, Nagoya University, Furo-cho, Chikusa-ku, Nagoya, Aichi 464-8603, Japan

[2] Department of Chemistry for Materials, Graduate School of Engineering, Mie University, 1577 Kurimamachiya-cho, Tsu, Mie 514-8507, Japan

[3]Department of Chemistry, College of Science, Rikkyo University, 3-34-1 Nishi-Ikebukuro, Toshima, Tokyo 171-8501, Japan

Corresponding Author:

 mhara@chembio.nagoya-u.ac.jp (M. H.) and tseki@chembio.nagoya-u.ac.jp (T. S.)

For Table of Contents use only

Humidity-induced self-assembly via ion aggregation
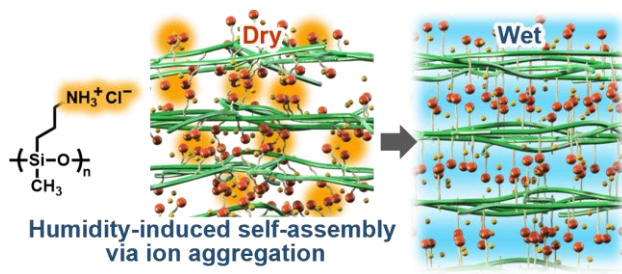
ABSTRACT:

Polysiloxanes exhibit practical properties not observed in carbon- or carbon-oxygen backbone polymers. Linear ionic polysiloxanes containing an amine hydrochloric salt exhibit a humidity-induced self-assembly (HiSA) behavior. HiSA leads to nanoscale structuring by the uptake of absorbed water around the ionic aggregates of the polymer, promoting the hydrophilic-hydrophobic phase separation of the polymer. The resulting polymer forms a self-assembled lamellar nanostructure with a period of ca. 1.6 nm. Herein we investigate the factors affecting the HiSA behavior. Introducing a dimethyl siloxane unit into the ionic polysiloxane achieves a more ordered lamellar structure and improves the nanostructure stability at higher humidities. The flexibility of the polysiloxane backbone, formation of ionic aggregates, and hydrophilic-hydrophobic phase separation affect the HiSA behavior. This nanoscale assembly can be characterized as a lyotropic liquid crystal formed with the assistance of ion aggregation instead of the hydrophobic effect in aqueous systems of ordinary surfactants.

INTRODUCTION

Polysiloxanes are found in highly functional materials in diverse fields because they exhibit practical properties not observed in carbon- or carbon-oxygen backbone polymers.[1–7] These include flexibility, biocompatibility, weather resistance, gas permeability, and transparency. Polysiloxanes with a network structure are used as the inorganic components of organic-inorganic composite materials. Combining silica and polysiloxane networks with a liquid crystalline template serves as a framework for various mesoporous materials.[8–14] On the other hand, the high

3

flexibility of linear polysiloxanes induces an amorphous state at room temperature. Linear polysiloxanes are used in oils, greases, and shampoos.[15–17] Moreover, introducing side chains with a high aggregation ability forms a self-assembled nanostructure of linear polysiloxanes at or above room temperature.[18–22] A similar phenomenon is observed in the case of block copolymers.[23,24]

In polymers and biomembranes, the balance between the hydrophilic and hydrophobic parts is responsible for the self-assembled lamellar nanostructures. Most studies on this topic use carbon-backbone polymers. Very recently, we reported that introducing an ammonium salt into all monomer units of the polysiloxane self-assembles to form a nanoscale lamellar structure without a long chain or mesogen.[25] Interestingly, this linear polysiloxane in a dry state exhibits an elastic modulus and strong adhesive properties comparable to those of carbon-backbone resins.

Herein we investigate factors affecting the formation of the lamellar nanostructure. Specifically, we examine the influences of the backbone nature, environmental humidity, degree of neutralization (ionic state), and the introduction of a hydrophobic dimethylsiloxane (DMS) unit in the backbone. Nanostructure formation is a characteristic of the polysiloxane backbone. Humidity plays a role in nanostructure ordering. Although humidity-induced self-assembly (HiSA) of carbon backbone-based polymers have been explored as functional materials for proton conduction[26] and humidity-responsive liquid crystal polymer actuators,[27,28] the optimal conditions for HiSA of flexible linear polysiloxanes have yet to be elucidated. Nanostructure formation in our linear polysiloxanes should be based on the lyotropic liquid crystallinity and ion aggregation. This mechanism differs from typical lyotropic liquid crystals where aggregation occurs via a hydrophobic effect,[29–31] a rigid and hydrophobic core with hydrophilic groups at the peripheries via a π-stack effect[26,29,32] steric hindrance effect,[33] or hydrogen-bonding interaction.[34,35]

EXPERIMENTAL SECTION

Chart 1 shows the effect of the degree of neutralization of a linear polysiloxane using the PAmMS$_n$ series. The subscript n represents the degree of neutralization. For example, PAmMS$_{100}$ indicates a polymer with 100% neutralization (salt form). A PAmMS$_{1-x}$-*co*-PDMS$_x$ series and a carbon-backbone polymer with a similar ammonium side group (PDMAMA-HCl) were used to verify the influence of introducing the DMS unit and the effect of the main chain structure, respectively.
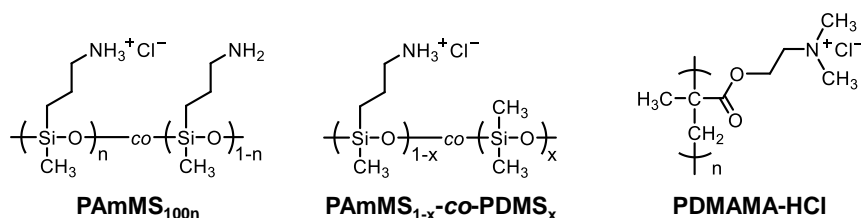
Chart 1. Chemical structures of the polymers.

PAmMS$_{100}$ was synthesized via the hydrolysis and polycondensation of 3-aminopropyldimethoxymethylsilane in a hydrochloric acid aqueous solution according to the previous report.[25] PAmMS$_{100}$ showed $M_n=3.2\times10^3$ and $M_w/M_n=3.67$. To prepare polysiloxanes with other degrees of neutralization, non-neutralized polysiloxane (PAmMS$_0$) was synthesized.[25] Although size exclusion chromatography (SEC) analysis of the resulting PAmMS$_0$ was difficult due to the strong interaction with the SEC column, the spectra of matrix assisted laser desorption/ionization time-of-flight mass spectrometry (MALDI-TOF-MS) showed that PAmMS$_0$ had the same molecular weight and distribution as PAmMS$_{100}$ (see SI). Adjusting the molar mixing

ratio of hydrochloric acid varied the degree of neutralization in the polysiloxanes. Neutralized polysiloxanes containing the DMS unit were synthesized by mixing 3-aminopropyldimethoxymethylsilane and dimethyldimethoxysilane in a hydrochloric acid solution.

Approximately 300-nm-thick spin-cast films of these polymers were prepared on a glass slide. Grazing-incidence small-angle X-ray scattering [GI-SAXS; FR-E (Rigaku)] and X-ray reflectivity [XRR; ATX-G (Rigaku)] measurements under controlled humidity characterized their structures. The humidity was controlled using a precise dew-point generator me-40DP series (Micro Equipment). A temperature and humidity recorder using an RTR-503 (T&D) monitored the humidity in the sample chamber. The supporting information provides details of the synthesis, characterizations, and measurements.

RESULTS AND DISCUSSION

Figure 1a shows the GI-SAXS images at a relative humidity (RH) of 30% for a PAmMS$_{100}$ film. The out-of-plane direction of the substrate shows two scatterings. The scatterings correspond to periods of 1.63 nm and 0.82 nm. They are assigned to the 001 and 002 planes of the lamellar structure from the ratio of the *d*-values, respectively. According to a molecular modeling, the side group length of the monomer is approximately 0.8 nm. The assumption of bilayer stacked structure well explains the lamella spacing (Supporting Information). Figure 1b depicts the formation of the periodic structure in which the methyl group covers the free surface (air interface). Covering the air interface arranges the main chain and side group orientations of the polysiloxane to neatly laminate the lamellar structure onto the substrate.
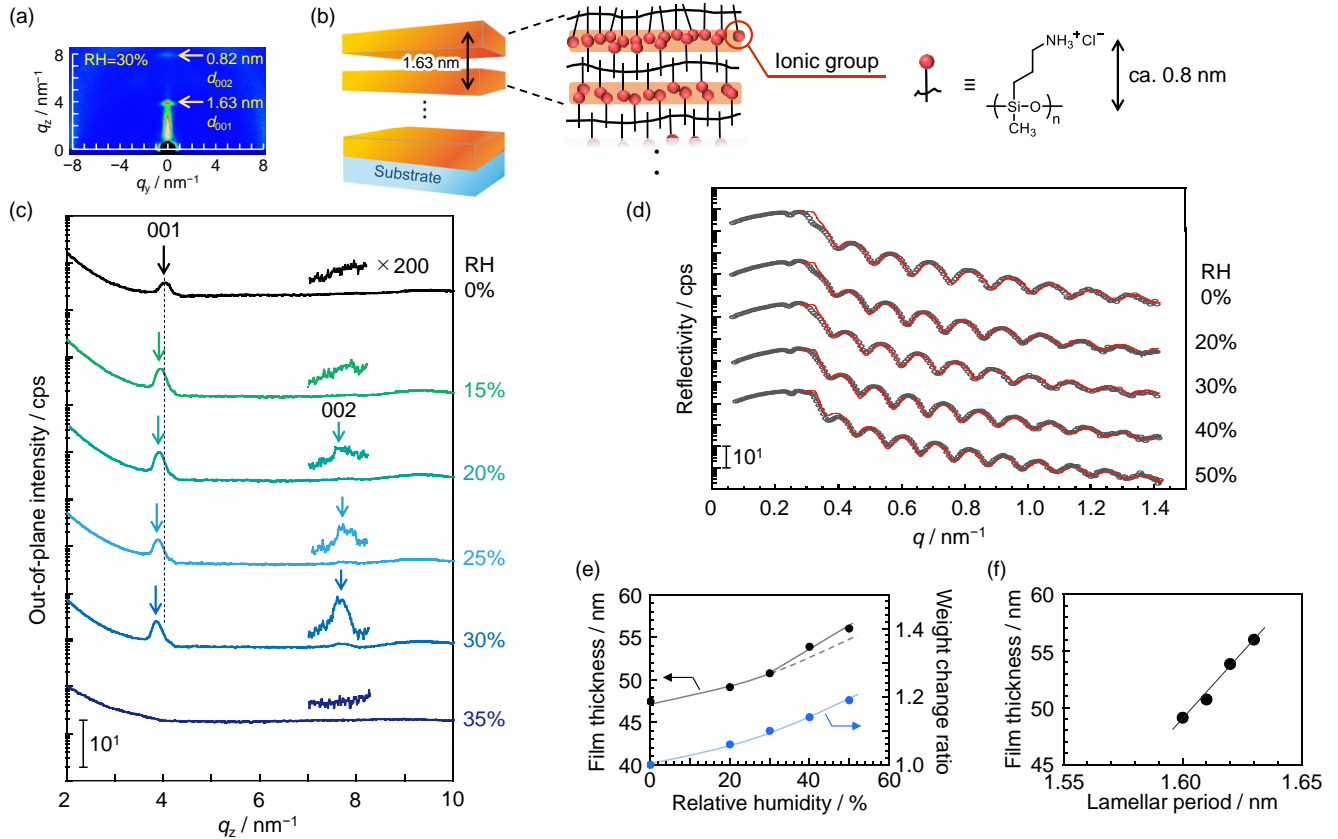
Figure 1. (a) GI-SAXS image and (b) the structural model of a $PAmMS_{100}$ film at RH=30%. (c) Out-of-plane intensity profiles from humidity-controlled GI-SAXS measurements of $PAmMS_{100}$ films. Insets show magnified data (200 times) of the scattering intensity derived from the 002 plane. (d) Humidity-controlled XRR profiles of the $PAmMS_{100}$ film from experimental data (gray) and fitting simulation (red). (e) Thickness and weight change ratio changes of the $PAmMS_{100}$ film with humidification. Weight change ratio data is from reference 25. Gray dashed line shows the trace of the weight change ratio of the film based on the data at lower RHs. (f) Relationship between the lamellar period and film thickness of $PAmMS_{100}$ film.

Figure 1c plots the out-of-plane intensity profiles obtained by GI-SAXS measurements upon increasing the humidity starting from the dry state (RH=0%). At RH=0 and 15%, the lamellae exhibit only primary scattering. Humidification sharpens the primary scattering and secondary scattering appears. Magnification (200-fold) of the secondary scattering shows that the lamellar

structure is mostly ordered at RH=30% (Fig. 1c, insets). The primary scattering shifts to a low q region with humidification, indicating that the lamellar spacing increases from 1.56 nm (RH=0%) to 1.63 nm (RH=30%).

This polymer exhibits hygroscopicity.[25] The lamellar spacing increases as the absorbed water increases. Lamellar scattering abruptly disappears at RH=35%, indicating that the lamellar structure dissolves in the presence of water above RH~35%. This easy dissolution indicates that layer structuring is assisted by an attractive force due to ion aggregates and that the hydrophobic siloxane backbone cannot form a layer. However, a definite nanoscale layer structure is formed under optimum humidity conditions. This is a unique characteristic of our present system.

Several reports have introduced ionic groups into all monomer units of linear polysiloxanes. However, these studies focused on functions such as ion conductivity,[36,37] dielectric,[38] and antimicrobial properties.[39] Hence, nanostructure formation via self-assembly under humidification has not received much attention. The same polysiloxane in this work was used to investigate an ionic self-assembling complex unit with liquid crystal mesogens,[40] but the self-assembly of the polysiloxane itself was not studied. It should be noted that the self-assembly process can be regarded as a new phenomenon, which does not require a long chain or mesogen. Therefore, this humidity-induced phenomenon can becalled HiSA. Rigid ladder polysiloxanes containing ionic groups in all monomer units form hexagonal structures instead of lamellae, which are stable over RH=80%.[41] The main chain rigidity may lead to the difference in the morphology and stability of the HiSA structure.

Figure 1d shows the XRR profiles of this film. The fringe period becomes shorter as the humidity increases, suggesting that the film thickness increases as the humidity increases. The film

thickness calculated from the fitting simulation is shown in Fig. 1e. We have previously investigated the change in polymer weight with humidification (Fig. 1e, light blue circles).[25] The increased polymer weight can be regarded as the amount of water adsorbed. The increment of the water adsorption and the increased film thickness are well correlated up to RH=30%. However, the increase in film thickness exceeds the increase in water absorption above RH=35% (Fig. 1e, auxiliary dashed line).

This deviation may be related to the dissolution of the lamellar structure above RH=35%, as indicated by the GI-SAXS measurements (Fig. 1c). We assume that the dissolution of the lamellar structure is accompanied by an increase in the free volume of $PAmMS_{100}$ due to the loss of the ordered structure, which leads to the increased film thickness. The XRR measurements indicate that the film thickness of the lamellar structure shows a linear correlation with the lamellar spacing (Fig. 1f). This observation suggests that the hygroscopic water is selectively incorporated between the lamellar layers in the humidified region.

Some of the profiles in the low q region do not agree with the experimental results (Fig. 1d). This deviation probably may arise from the assumption in the fitting that the film has a uniform density in the depth direction. It is reasonable that the free surface of the polymer film has a higher mobility than the inner part of the film, and the polymer chain in contact with the substrate has an even lower mobility.[42−44] Polymer films tend to show a density gradient in the depth direction.

A methacrylate polymer with a similar side chemical structure was used to assess the role of the polysiloxane main chain in nanostructure formation. GI-SAXS measurements under various humidity conditions were made for a polymethacrylate containing ammonium salt PDMAMA-HCl (Chart 1), which was fully neutralized poly[2-(dimethylamino)ethyl methacrylate] (Tokyo

Chemical Industry, M_w: 25,000) using hydrochloric acid. PDMAMA-HCl exhibits the same or higher hygroscopicity as $PAmMS_{100}$ (Fig. 2a).[25] In contrast, characteristic scattering is not observed under any humidity conditions up to 90% (Fig. 2b), indicating that PDMAMA-HCl does not form the HiSA structure. Thus, main chain flexibility of $PAmMS_{100}$ should be important for HiSA nanostructure formation.
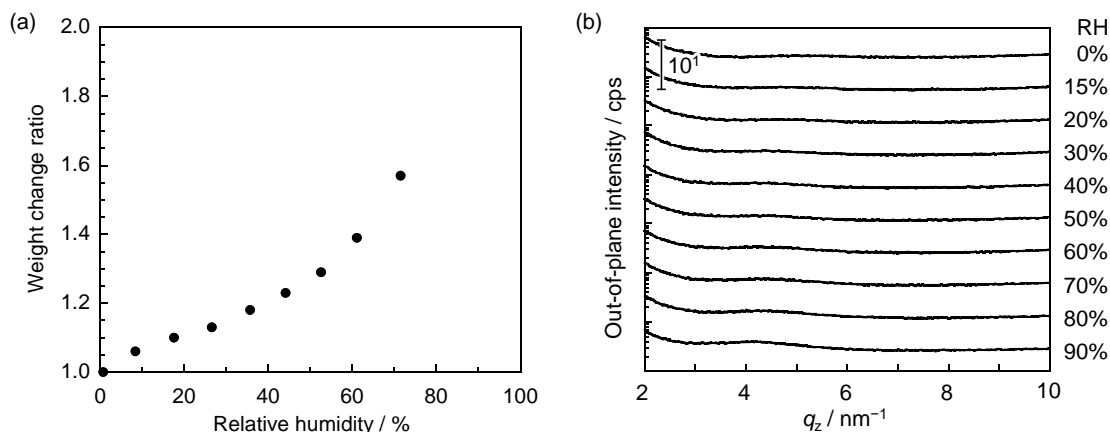
Figure 2. (a) Weight change ratio of polymethacrylate containing an ammonium salt. (b) Out-of-plane intensity profiles obtained by humidity-controlled GI-SAXS measurements of polymethacrylate.

Next, GI-SAXS profiles of the linear polysiloxanes were measured for different degrees of neutralization. HiSA is observed in $PAmMS_{75}$ (75% neutralization). It shows the highest lamellar structure order at RH=20%, and the scattering peak intensity decreases at a higher humidity (Fig. 3a). As observed for $PAmMS_{100}$, the scattering peaks shift to the lower q region and the lamellar spacing increases as the humidity increases.

Figure 3c depicts the relationship between humidity and lamellar spacing. The lamellar structure of $PAmMS_{75}$ dissolves at RH=30%, while that of $PAmMS_{100}$ dissolves at RH=35%. For $PAmMS_{60}$ (60% neutralization), scattering is not observed under any humidity condition (Fig. 3b).

These results indicate that polysiloxane with a degree of polymer neutralization provides a more ordered lamellar structure. Additionally, the optimum humidity conditions for lamellar structure ordering depend on the degree of neutralization.

Figure 3d shows the humidity response of the lamellar structure. At a low humidity, strong ion aggregates are formed (i).[45] The lamellar structure does not have a well-developed order due to the size distribution of the ion aggregates. The lamellar spacing at this time is defined as d_1. When water is incorporated into the film via humidification, it acts as a plasticizer and relaxes the ion aggregates (ii). In this situation, nanophase separation between the hydrophilic and hydrophobic regions becomes clear. The order of the lamellar structure is improved. Then the lamellar spacing d_2 becomes wider than d_1 because hygroscopic water is incorporated into the ion aggregation sites. Further humidification (RH > 30%) hydrates the polymer and destroys the lamellar structure (iii). Dasgupta et al. reported that introducing a rigid structure into polysiloxane leads to the development of regular structures.[46] We assume that the increased degree of neutralization enhanced the rigidity in our material. The lamellar spacing of $PAmMS_{100}$ is shorter than that of $PAmMS_{75}$ (Fig. 3c) because a higher neutralization level strengthens the ionic aggregation between the layers.
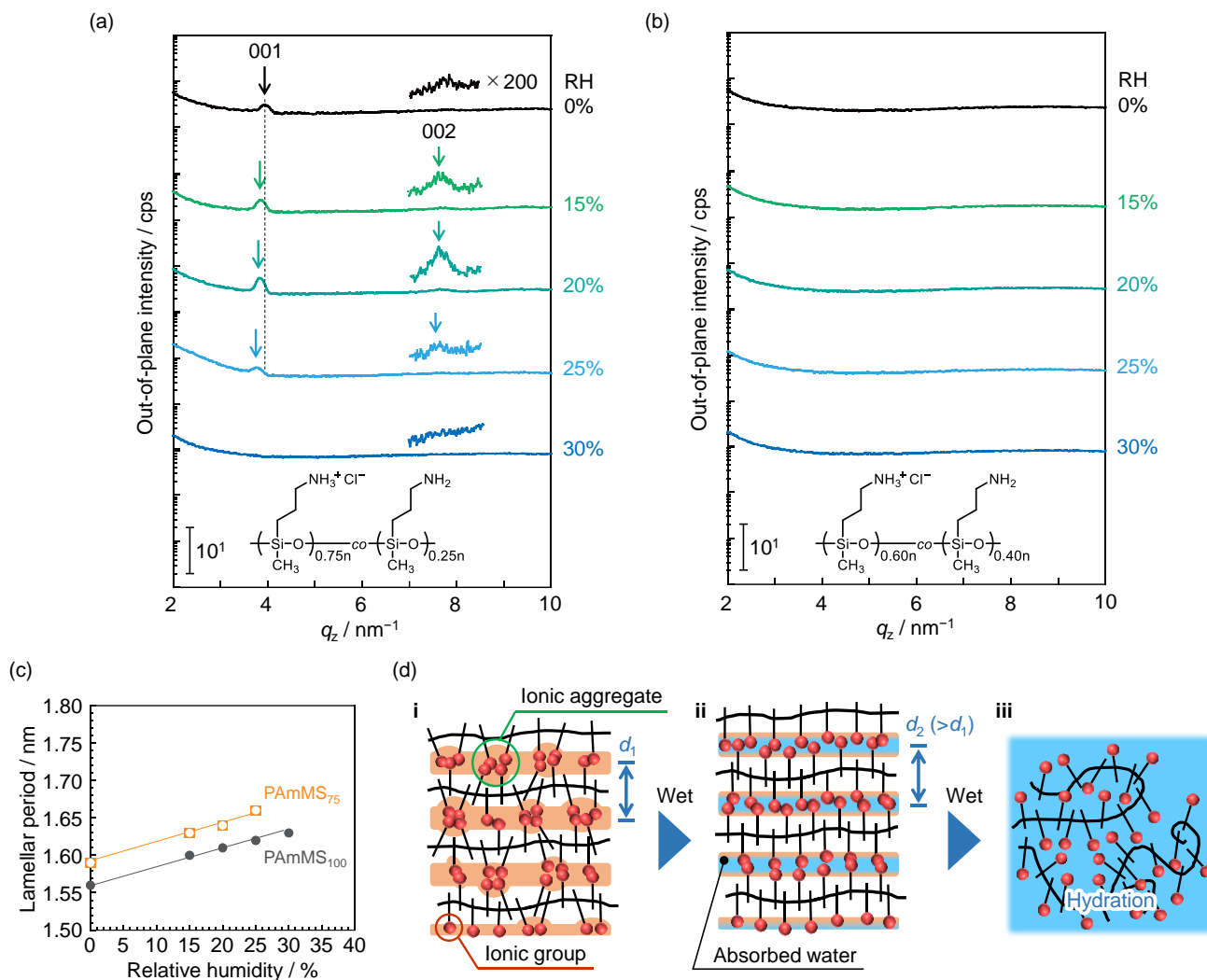
Figure 3. Out-of-plane intensity profiles obtained by humidity-controlled GI-SAXS measurements of PAmMS$_{75}$ (a) and PAmMS$_{60}$ (b) films. (c) Relationship between the relative humidity and lamellar period. (d) Changes in the plausible lamellar structure with humidification.

Next, we modified the main chain structure of polysiloxanes by partly replacing PAmMS$_{100}$ with DMS units, which is denoted as PAmMS$_{1-x}$-co-PDMS$_x$ (Chart 1). The subscript x in the chemical formula indicates the molar fraction of the DMS unit, which was evaluated from the ^{1}H NMR data. The synthesis procedures are described in the supporting information. Table 1 summarizes the copolymerization ratio, M_n, and glass transition temperature (T_g).

Table 1. Molecular mass[a] and glass transition temperature[b] data of PAmMS-*co*-PDMS series.

label	M_n	M_w/M_n	T_g / °C
PAmMS	6.5×10^3	1.86	117
PAmMS$_{0.93}$-*co*-PDMS$_{0.07}$	5.3×10^3	1.84	79
PAmMS$_{0.85}$-*co*-PDMS$_{0.15}$	7.3×10^3	2.44	63
PAmMS$_{0.70}$-*co*-PDMS$_{0.30}$	8.0×10^3	2.62	55
PAmMS$_{0.51}$-*co*-PDMS$_{0.49}$	1.2×10^4	3.35	42

[a]M_n and M_w/M_n are evaluated by SEC measurements. All samples are bimodal. An additional peak (M_n 1.0×10^3, M_w/M_n 1.06) is observed.
[b]T_g is determined by DSC measurements.

Figure 4a shows the out-of-plane intensity profiles obtained by the GI-SAXS measurements of PAmMS$_{1-x}$-*co*-PDMS$_x$ spin-cast films. The scattering peaks become sharper, and secondary scattering is observed by copolymerization with DMS. Introducing the DMS unit clearly improves the lamellar structure order. The lamellar spacing also increases as the humidity increases (Fig. 4b). Additionally, the spacing increases with increasing x (Fig. 4c). Note that in the two samples (x=0.15 and 0.30), a shoulder was observed on the wide-angle side of the primary peak during the humidification process. This should be of experimental artifact and not originated from two periods of structure. At a particular incident angle, the transmission and reflection peaks are separately observed on the humidification process[47,48].

Although the water adsorption decreases as the DMS unit increases (Fig. 4c, weight change ratio), the lamellar spacing increases. Figure 4e depicts this behavior. If half of the ionic units are

replaced with DMS units, for example, from $PAmMS_{100}$ (I), we can draw the model shown in II. In this state, the ionic groups are separated from each other, making it difficult to form ion aggregates. Therefore, the siloxane main chain should fold for the favorite formation of ion aggregates, and the lamellar spacing D_2 becomes larger than D_1 (III).

Another feature of HiSA with DMS units is that the moisture resistance (stability of the nanostructure at higher humidities) improves with increasing x (Fig. 4d). The introduction of the DMS unit decreases the solubility in water because water adsorption promotes the nanophase separation ability between the hydrophilic and hydrophobic regions. It is assumed that the introduction of the DMS units lowers the material rigidity, but the ordering of the lamellar structure is improved. This suggests that the hydrophilic-hydrophobic balance is also an important parameter for self-assembling structuring.
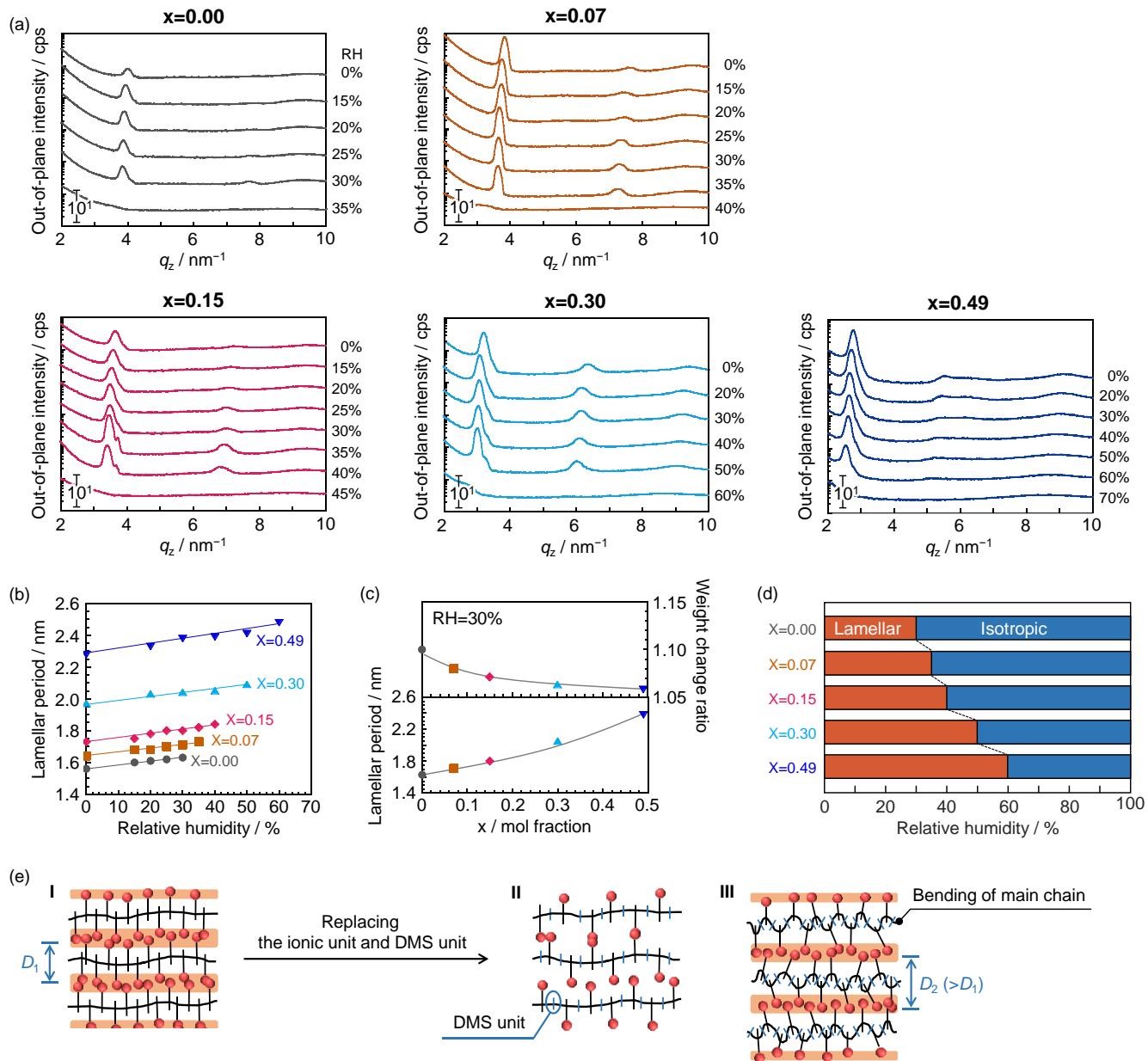
Figure 4. (a) Out-of-plane intensity profiles obtained by humidity-controlled GI-SAXS measurements of PAmMS$_{1-x}$-*co*-PDMS$_x$ films. (b) Lamellar period with humidification as a function of *x*. (c) Adsorbed water amount and lamellar period with the introduction of DMS units at RH=30%. "Weight change ratio" values show the relative change in weight at RH=0%. (d) Phase transition point with RH as a function of *x*. (e) Plausible structural model when the ionic units of polysiloxane are replaced by DMS units. Depiction of adsorbed water is omitted for simplicity.

CONCLUSIONS

In summary, we investigated the HiSA behavior of linear polysiloxanes containing alkylamine hydrochloride side chains in detail to elucidate the influence of the backbone structure (polysiloxane or polymethacrylate), the degree of neutralization, and the copolymerization content of DMS. The formation of the lamellar structure is a characteristic of the flexible polysiloxane backbone. Both the degree of neutralization and the copolymerization ratio of DMS affect the nanoscale structuring properties. The HiSA phenomenon can be regarded as an extended category of lyotropic liquid crystals. In our polysiloxanes, ionic aggregation is critical for the formation of the lyotropic liquid crystalline phases. Therefore, we propose a new aspect of lyotropic liquid crystals, which differs from the formation mechanism of the conventional lyotropic liquid crystals based on the hydrophobic effect. Since varying the silane coupling agents and neutralizing salts can change the design of linear polysiloxanes, this material approach is a suitable strategy to accumulate knowledge about the HiSA behavior. Understanding of the HiSA behavior should realize new functionalization tools for humidity-driven devices. Studies on the nanostructure formation and the humidity-dependent mechanical property are in progress because the nanostructure should be essential for the unique humidity-dependent mechanical property in $PAmMS_{100}$.[25]

Competing interests

The authors declare no competing interests.

Supporting information

The Supporting Information is available free of charge at https://doi.org.

Additional experimental details, materials, methods, and measurements: synthetic recipe and characterization of siloxane copolymers; Table S1: MALDI-TOF mass spectra of linear polysiloxane; Figure S1: ^{1}H NMR spectra and SEC charts of siloxane copolymers: Figure S2−4:

ORCID

Mitsuo Hara: 0000-0003-1829-5153

Yoshihisa Fujii 0000-0001-9419-8537

Shusaku Nagano: 0000-0002-3929-6377

Takahiro Seki: 0000-0003-3010-2641

REFERENCES

1. Clarson, S. J.; Fitzgerald, J. J.; Owen, M. J.; Smith, S. D., Eds.; *Silicones and Silicone-Modified Materials*, American Chemical Society, 2000.

2. Abbasi, F.; Mirzadeh, H.; Katbab, A.-A. Modification of polysiloxane polymers for biomedical applications: A review. *Polym. Int.* **2001**, *50*, 1279−1287.

3. Eduok, U.; Faye, O.; Szpunar, J. Recent developments and applications of protective silicone coatings: A review of PDMS functional materials. *Prog. Org. Coat.* **2017**, *111*, 124−163.

4. Pouget, E.; Tonnar, J.; Lucas, P.; Lacroix-Desmazes, P.; Ganachaud, F.; Boutevin, B. Well-architectured poly(dimethylsiloxane)-containing copolymers obtained by radical chemistry. *Chem. Rev.* **2010**, *110*, 1233−1277.

5. Mark, J. E. Some Interesting Things about Polysiloxanes. *Acc. Chem. Res.* **2004**, *37*, 946−953.

6. Ariga, K.; Yamauchi, Y.; Mori, T.; Hill, J. P. 25th Anniversary Article: What Can Be Done with the Langmuir-Blodgett Method? Recent Developments and its Critical Role in Materials Science. *Adv. Mater.* **2013**, *25*, 6477−6512.

7. Miwa, Y.; Taira, K.; Kurachi, J.; Udagawa, T.; Kutsumizu, S. A gas-plastic elastomer that quickly self-heals damage with the aid of CO_2 gas. *Nat. Commun.* **2019**, *10*, 1828.

8. Simon, P. F. W.; Ulrich, R.; Spiess, H. W.; Wiesner, U. Block Copolymer-Ceramic Hybrid Materials from Organically Modified Ceramic Precursors. *Chem. Mater.* **2001**, *13*, 3464−3486.

9. Wan, Y.; Zhao, D. On the Controllable Soft-Templating Approach to Mesoporous Silicates. *Chem. Rev.* **2007**, *107*, 2821−2860.

10. Alothman, Z. A. A Review: Fundamental Aspects of Silicate Mesoporous Materials. *Materials* **2012**, *5*, 2874−2902.

11. Ariga, K.; Vinu, A.; Yamauchi, Y.; Ji, Q.; Hill, J. P. Nanoarchitectonics for Mesoporous Materials, *Bull. Chem. Soc. Jpn.* **2012**, *85*, 1−32.

12. Hara, M.; Orito, T.; Nagano, S.; Seki, T.; Humidity-responsive phase transition andon-demand UV-curing in a hygroscopicpolysiloxane-surfactant nanohybrid film. *Chem. Commun.* **2018**, *54*, 1457−1460.

13. Hara, M. Mesostructure and orientation control of lyotropic liquid crystals in a polysiloxane matrix. *Polym. J.* **2019**, *51*, 989−996.

14. Hara, M.; Wakitani, N.; Kodama, A.; Nagano, S.; Seki, T. Hierarchical Photocomposition of Heteronanostructures in a Surfactant-Polysiloxane Hybrid Film toward Next-Generation Nanolithography. *ACS Appl. Polym. Mater.* **2020**, *2*, 2284−2290.

15. Zeigler, J. M.; Fearon, F. W. G., Eds., *Silicon-Based Polymer Science: A Comprehensive Resource*, American Chemical Society, 1989.

16. Rahimi, A.; Shokrolahi, P. Application of inorganic polymeric materials I. Polysiloxanes. *Int. J. Inorg. Mater.* **2001**, *3*, 843−847.

17. Dewasthale, S.; Andrews, C.; Graiver, D.; Narayan, R. Water Soluble Polysiloxanes. *Silicon* **2017**, *9*, 619−628.

18. Kumar, U.; Kato, T.; Fréchet, J. M. Use of intermolecular hydrogen bonding for the induction of liquid crystallinity in the side chain of polysiloxanes. *J. Am. Chem. Soc.* **1992**, *114*, 6630−6639.

19. Yao, W.; Gao, Y.; Yuan, X.; He, B.; Yu, H.; Zhang, L.; Shen, Z.; He, W.; Yang, Z.; Yang, H.; Yang, D. Synthesis and self-assembly behaviours of side-chain smectic thiol-ene polymers based on the polysiloxane backbone. *J. Mater. Chem. C* **2016**, *4*, 1425−1440.

20. Zha, R. H.; de Waal, B. F. M.; Lutz, M.; Teunissen, A. J. P.; Meijer, E. W. End Groups of Functionalized Siloxane Oligomers Direct Block-Copolymeric or Liquid-Crystalline Self-Assembly Behavior. *J. Am. Chem. Soc.* **2016**, *138*, 5693−5698.

21. Ishiwari, F.; Okabe, G.; Ogiwara, H.; Kajitani, T.; Tokita, M.; Takata, M.; Fukushima, T. Terminal Functionalization with a Triptycene Motif That Dramatically Changes the Structural and Physical Properties of an Amorphous Polymer. *J. Am. Chem. Soc.* **2018**, *140*, 13497−13502.

22. Li, X.; Chang, X.; Zheng, X.; Kong, W.; Zhuang, Y.; Yan, G.; Meng, F. Self-assembly, liquid crystalline behavior and electrorheological performance of phthalocyanine-contaning polysiloxanes, *Eur. Polym. J.* **2021**, *150*, 110417.

23. Kim, H.-C.; Park, S.-M.; Hinsberg, W. D. Block Copolymer Based Nanostructures: Materials, Processes, and Applications to Electronics. *Chem. Rev.* **2010**, *110*, 146−177.

24. Cummins, C.; Ghoshal, T.; Holmes, J. D.; Morris, M. A. Strategies for Inorganic Incorporation using Neat Block Copolymer Thin Films for Etch Mask Function and Nanotechnological Application. *Adv. Mater.* **2016**, *28*, 5586−5618.

25. Hara, M.; Iijima, Y.; Nagano, S.; Seki, T. Simple linear ionic polysiloxane showing unexpected nanostructure and mechanical properties. *Sci. Rep.* **2021**, *11*, 17683.

26. Krishnan, K.; Iwatsuki, H.; Hara, M.; Nagano, S.; Nagao, Y. Proton conductivity enhancement in oriented, sulfonated polyimide thin films. *J. Mater. Chem. A* **2014**, *2*, 6895−6903.

27. de Haan, L. T.; Verjans, J. M. N.; Broer, D. J.; Bastiaansen, C. W. M.; Schenning, A. P. H. J. Humidity-Responsive Liquid Crystalline Polymer Actuators with an Asymmetry in the Molecular Trigger That Bend, Fold, and Curl. *J. Am. Chem. Soc.* **2014**, *136*, 10585−10588.

28. Liu, Y.; Xu, B.; Sun, S.; Wei, J.; Wu, L.; Yu, Y. Humidity- and Photo-Induced Mechanical Actuation of Cross-Linked Liquid Crystal Polymers. *Adv. Mater.* **2017**, *29*, 1604792.

29. Ringsdorf, H.; Schlarb, B.; Venzmer, J. Molecular Architecture and Function of Polymeric Oriented Systems: Models for the Study of Organization, Surface Recognition, and Dynamics of Biomembranes. *Angew. Chem. Int. Ed.* **1988**, *27*, 113−158.

30. Israelachvili, J. N. Intermolecular and Surface Forces with Applications to Colloidal and Biological Systems; Academic: London, **1985**, 249−257.

31. Wanka, G.; Hoffmann, H.; Ulbricht, W. Phase Diagrams and Aggregation Behavior of Poly(oxyethylene)-Poly(oxypropylene)-Poly(oxyethylene) Triblock Copolymers in Aqueous Solutions. *Macromolecules* **1994**, *27*, 4145−4159.

32. Lydon, J. Chromonic review. *J. Mater. Chem.* **2010**, *20*, 10071−10099.

33. Varshney, S. K. Liquid Crystalline Polymers: A Novel State of Material. *J. Macromol. Sci., Polym. Rev.* **1986**, *26*, 551−650.

34. Kato, T.; Mizoshita, N.; Kishimoto, K. Functional Liquid-Crystalline Assemblies: Self-Organized Soft Materials. *Adv. Mater.* **2006**, *45*, 38−68.

35. Uchida, J.; Soberats, B.; Gupta, M.; Kato, T. Advanced Functional Liquid Crystals. *Adv. Mater.* **2022**, 2109063.

36. Kang, J.-J.; Li, W.-Y.; Lin, Y.; Li, X.-P.; Xiao, X.-R.; Fang, S.-B. Synthesis and ionic conductivity of a polysiloxane containing quaternary ammonium groups. *Polym. Adv. Technol.* **2004**, *15*, 61−64.

37. Jourdain, A.; Serghei, A.; Drockenmuller, E. Enhanced Ionic Conductivity of a 1,2,3-Triazolium-Based Poly(siloxane ionic liquid) Homopolymer. *ACS Macro Lett.* **2016**, *5*, 1283−1286.

38. Bocharova, V.; Wojnarowska, Z.; Cao, P.-F.; Fu, Y.; Kumar, R.; Li, B.; Novilov, V. N.; Zhao, S.; Kisliuk, A.; Saito, T.; Mays, J. W.; Sumpter, B. G.; Sokolov, A. P. Influence of Chain Rigidity and Dielectric Constant on the Glass Transition Temperature in Polymerized Ionic Liquids. *J. Phys. Chem. B* **2017**, *121*, 11511−11519.

39. Mizerska, U.; Fortuniak, W.; Chojnowski, J.; Hałasa, R.; Konopacka, A.; Werel, W. Polysiloxane cationic biocides with imidazolium salt (ImS) groups, synthesis and antivacterial properties. *Eur. Polym. J.* **2009**, *45*, 779−787.

40. Cheng, Z.; Liu, R.; Ren, B. Ionically Self-Assembled Thermotropic Liquid Crystalline Complexes of Linear Polysiloxane and Dendritic Amphiphiles. *J. Macromol. Sci., Part B: Phys.* **2012**, *51*, 1172−1185.

41. Kaneko, Y.; Toyodome, H.; Shoiriki, M.; Iyi, N. Preparation of Ionic Silsesquioxanes with Regular Structures and Their Hybridization. *Int. J. Polym. Sci.* **2012**, *2012*, 684278.

42. Kajiyama, T.; Tanaka, K.; Takahara, A. Study of the surface glass transition behaviour of amorphous polymer film by scanning-force microscopy and surface spectroscopy. *Polymer* **1998**, *39*, 4665−4673.

43. Xie, F.; Zhang, H. F.; Lee, F. K.; Du, B.; Tsui, O. K. C.; Yokoe, Y.; Tanaka, K.; Takahara, A.; Kajiyama, T.; He, T. Effect of Low Surface Energy Chain Ends on the Glass Transition Temperature of Polymer Thin Films. *Macromolecules* **2002**, *35*, 1491−1492.

44. Tanaka, K.; Tsuchimura, Y.; Akabori, K.; Ito, F.; Nagamura, T. Time- and space-resolved fluorescence study on interfacial mobility of polymers. *Appl. Phys. Lett.* **2006**, *89*, 061916.

45. Eisenberg, A.; Navratil, M. Ion Clustering and Viscoelastic Relaxation in Styrene-Based Ionomers. II. Effect of Ion Concentration. *Macromolecules* **1973**, *6*, 604−612.

46. Sarkar, A.; Negi, L. M. S.; Lewis, K. M.; Vasimalai, N.; Gowd, E. B.; Dasgupta, D. Microstructure Induced Rigidity of Polysiloxane Yielding Hierarchical Self-Assembly of Alkyl Side Chains. *Macromol. Chem. Phys.* **2019**, *220*, 1900408.

47. Komura, M.; Watanabe, K.; Iyoda, T.; Yamada, T.; Yoshida, H.; Iwasaki, Y. Laboratory-GISAXS Measurements of Block Copolymer Films with Highly Ordered and Normally Oriented Nanocylinders. *Chem. Lett.* **2009**, *38*, 408−409.

48. Ree, M. Probing the Self-Assembled Nanostructures of Functional Polymers with Synchrotron Grazing Incidence X-Ray Scattering. *Macromol. Rapid Commun.* **2014**, *35*, 930−959.